AD NUMBER

AD449823

LIMITATION CHANGES

TO:

Approved for public release; distribution is unlimited.

FROM:

**Distribution authorized to U.S. Gov't. agencies and their contractors;
Administrative/Operational Use; AUG 1964. Other requests shall be referred to Commander, US Army Missile Command, Attn: AMSMI-RAS, Redstone Arsenal, AL 35898-5244.**

AUTHORITY

RSIC ltr 5 Jan 1966

AD

449823

ARPA ORDER NO. 357-63
PROJECT CODE NO. 7400

Copy No 65

GENERAL MOTORS CORPORATION

TECHNICAL REPORT ON

MILLIMETER RADAR INSTRUMENTATION FOR STUDYING PLASMA EFFECTS ASSOCIATED WITH HYPERSONIC FLIGHT

H.M. Musal, Jr., R.I. Primich
W.E. Blore and P.E. Robillard

THIS RESEARCH WAS SUPPORTED BY THE
ADVANCED RESEARCH PROJECTS AGENCY
DEPARTMENT OF DEFENSE
AND WAS MONITORED BY THE
U.S. ARMY MISSILE COMMAND
REDSTONE ARSENAL, ALABAMA

GM DEFENSE RESEARCH LABORATORIES

SANTA BARBARA, CALIFORNIA

AEROSPACE OPERATIONS DEPARTMENT

CONTRACT NO. DA-04-495-ORD-3567(Z)
HYPERVELOCITY RANGE RESEARCH PROGRAM
A PART OF PROJECT "DEFENDER"

TR64-02J

DDC AVAILABILITY NOTICE
Qualified requesters may obtain copies of this report from DDC

AUGUST 1964

FOREWORD

The material presented in this report is a preprint of a paper to be presented at the First International Congress on Instrumentation in Aerospace Simulation Facilities, 28 – 29 September 1964 in Paris, France. The report is therefore printed in the format of the Congress.

The instrumentation described in this report is installed in the Flight Physics Range of GM Defense Research Laboratories, General Motors Corporation, and is used in an experimental research program investigating the flow-field variables associated with hypersonic-velocity projectiles in free flight under controlled environmental conditions. This research is supported by the Advanced Research Projects Agency under Contract No. DA-04-495-ORD-3567(Z).

The present report is one of a series of related papers covering various aspects of the above program. It is intended that this series of reports will provide a background of knowledge of the phenomena involved in the basic study, and will thus aid in a better understanding of the data obtained in the investigation.

CONTENTS

ILLUSTRATIONS

MILLIMETER RADAR INSTRUMENTATION FOR STUDYING PLASMA EFFECTS ASSOCIATED WITH HYPERSONIC FLIGHT*

H.M. Musal, Jr., R.I. Primich
W.E. Blore and P.E. Robillard

GM Defense Research Laboratories
General Motors Corporation
Santa Barbara, California, U.S.A.

Abstract

Millimeter wavelength radars are being used to study the plasma effects associated with the ionized flow fields of projectiles launched at hypersonic speeds into a free-flight ballistic range. Two CW doppler radars, which operate at frequencies of 35 and 70 Gc, are used to measure the nose-on backscattering radar cross sections of projectiles during their flight.

The design and performance of the two radars, which operate simultaneously through a wire-grid beam splitter, are described in detail. A doppler signal simulator provides absolute calibration of each radar so that the dynamic radar cross section of the projectile in flight can be measured to within ± one decibel.

The purpose of this millimeter radar instrumentation is to measure the changes that occur in the radar cross sections of hypersonic projectiles caused by their highly ionized flow fields. It has been observed that under certain conditions the nose-on backscattering radar cross section of a blunt-nosed metal projectile decreases drastically when a thin, shock-produced layer of ionized gas covers the projectile. A theoretical analysis of this effect is given. The details of the radar cross-section changes are intimately related to the spatial distribution of ionization in the bow-shock region. Comparisons between theoretical predictions and experimental data show good correlation.

I. INTRODUCTION

Millimeter wavelength radars are being used at GM Defense Research Laboratories to study the plasma effects associated with the ionized flow fields of projectiles launched at hypersonic speeds into a free-flight ballistic range under controlled environmental conditions. Two CW doppler radars, which operate at frequencies of 35 and 70 Gc, are used to measure the nose-on backscattering radar cross sections of projectiles during their flight at speeds up to 23,000 ft/sec through a chamber in which ambient pressures from one atmosphere down to 1 mm Hg can be maintained. The radars operate simultaneously with a common beam axis by the use of a wire-grid beam splitter. An important feature of each radar system is a doppler signal simulator, which provides absolute calibration of each radar so that the dynamic radar cross section of the projectile in flight can be measured to within ± one decibel relative to a square wavelength.

A specific experimental program in which the millimeter radars are currently being used is described here to illustrate their utilization. The purpose of this program is to measure the changes that occur in the radar cross sections of hypersonic projectiles caused by their highly ionized flow fields, and to relate these changes to the flow-field properties. It has been observed[1, 2] that under certain conditions the nose-on backscattering radar cross section of a blunt-nosed metal projectile decreases drastically when a thin shock-produced layer of ionized gas covers the projectile. A theoretical analysis of this effect is given here. It is shown that a thin layer of overdense plasma spreading from the stagnation point around the nose of the projectile causes electromagnetic diffraction and absorption, both of which decrease the backscattered electromagnetic power. The details of the resultant radar cross-section changes are intimately related to the spatial distribution of ionization in the bow-shock region, and hence are a sensitive indicator of the flow-field properties. Comparisons between the predictions of the theory presented here and experimental data obtained in the GM DRL ballistic range show good correlation.

II. DESCRIPTION OF RADARS

General Discussion

An artist's impression of the installation of the two radars on the ballistic range is shown in Figure 1. The two radars are permanently installed for simultaneous operation with a common beam axis. The antenna beams from the

*Part of the work described in this paper was sponsored by the Advanced Research Projects Agency, Department of Defense, U.S.A., Contract No. DA-04-495-ORD-3567(Z) as part of project "Defender". Related corporation-funded research conducted at GM DRL is also described.

two individual radar antennas are combined by a wire grid. This wire grid transmits the 70 Gc beam, which is polarized perpendicular to the wires, and reflects the 35 Gc beam, which is polarized parallel to the wires. The resultant coaxial beams from the two antennas of the two radars are directed through a dielectric window into an 8-foot-diameter ballistic-range tank. They are then deflected uprange by means of an expendable radar reflector centered on the flight axis. The backscattered signals (at the two frequencies) from the projectile, which are "doppler shifted" due to the projectile motion, propagate back along the same paths to the radar antennas. It has been found that mutual interference between the two radars is negligible. The doppler-shifted signals are detected and recorded. The magnitude of each signal, at any instant, is a measure of the radar cross section of the projectile at that particular range. The system is calibrated by transmission of a signal of known power and frequency from a known distance along the axis, which simulates in all respects a backscattered signal from a projectile in flight.

The CW doppler technique has been adopted for a number of reasons. The doppler shift in the frequency of the backscattered signal from the projectile is of sufficient magnitude to make it possible to use the doppler technique as a means of discriminating against the stationary background signal. A combination of CW nulling techniques, together with a simple band-pass amplifier, has been found to be very effective in the isolation of the doppler signal from the stationary background signal. Because of the large doppler shift (due to the high projectile velocity), it is quite practical to use a single klystron both as a transmitter and as a local oscillator. In addition, since the doppler shift is used to discriminate against unwanted background signals, a single antenna for both transmission and reception can be used. The resulting unit is simple to construct, operate, and maintain.

With CW operation of the radar, it is a simple matter to calibrate the radar accurately by the use of a phase-locked simulator.

The main disadvantage of a CW doppler radar, namely the absence of range resolution, is unimportant in the present application. The exact location of the projectile at any instant of time is determined by spark-shadowgraph chronograph stations along the length of the ballistic range.

The choice of radar frequency is governed primarily by two factors. First, it is important to minimize the angular spread of the radar beam so that interference from multiple reflected signals caused by the presence of the walls of the firing range is reduced as much as possible. Primich[3] has shown that, for practical dimensions of evacuated ballistic ranges (diameters of not less than 6 feet), the radar frequency should be above 30 Gc. This ensures a useful operating range, free from interference, of about 30 feet. Second, the radar frequency should be near the plasma frequency of the ionized flow field in order to maximize the radar-plasma interaction. Reference to stagnation-point plasma frequencies (see, for instance, Musal[4]) indicates that radar frequencies throughout the entire microwave spectrum up to 3,000 Gc are of interest. With these considerations in mind, an initial choice of 35 and 70 Gc for the radar frequencies was made.

In the type of study for which these radars are intended, it is of interest to compare the dynamic radar cross section of a body due to plasma effects to the radar cross section of the body in the absence of ionization. The latter is most conveniently measured in a conventional model radar range. In this instance there is no need to scale the body size, since the radar cross section can be measured directly before launching provided that a static radar range which operates at the same frequency as the doppler radar is available. For this reason a static radar range with both 35 and 70 Gc radars has been constructed to complement the dynamic radar measurement equipment. This equipment has been described elsewhere.[5]

35 Gc Radar System

A block diagram of the 35 Gc radar head is shown in Figure 2, and details may also be seen in the photograph of Figure 6. The circuit is basically a balanced bridge. The heart of the bridge is a hybrid T which allows a single antenna to be used for both transmission and reception. The background signal is partially cancelled by tuning the bridge. Provision is made to monitor the frequency and power radiated. In addition, part of the transmitter signal is used to provide local oscillator power in the balanced mixer.

The antenna is a right-circular conical horn with lens correction to provide maximum gain for that aperture size. The gain is approximately 30 decibels and the beamwidth is about 6 degrees.

The doppler amplifier is a straightforward video amplifier with a flat passband from 0.5 Mc to 6 Mc. At 35 Gc the doppler frequencies range from 0.7 Mc to 1.4 Mc for velocities from 10,000 to 20,000 feet per second. The gain of the doppler amplifier is approximately 30 decibels. The doppler signal output of the doppler amplifier is fed to two dual-beam oscilloscopes equipped with cameras to record the traces. Arrangements are made to view the entire flight and parts of the flight. At least one channel is

used to record a short section of flight in which the individual cycles of the doppler signal are visible.

Radar calibration, which is necessitated by the requirement for absolute radar cross-section measurements, is accomplished with the aid of the doppler signal simulator. The reflex klystron in the simulator is phase locked to the 35 Gc transmitter frequency at a variable offset frequency. By setting the offset frequency equal to the expected doppler frequency and by varying the power output of the simulator to obtain a curve of simulated power versus radar voltage output, a complete calibration of the radar can be obtained. The simulator can also be used to measure the frequency response and sensitivity of the radar receiver and the conversion loss of the mixer crystals. With the simulator antenna on the flight axis of the projectile, the free-space path loss can be measured to check the alignment of the radar reflector and antenna.

A block diagram of the 35 Gc doppler simulator is shown in Figure 3. A 35 Gc reference signal from the transmitter klystron is fed into a balanced crystal modulator. With the modulator tuned to suppress the original carrier, the modulator output frequencies are $35,000 \pm (30 + f_d)$ Mc, where $(30 + f_d)$ Mc is the modulation frequency and f_d is the simulated dopper frequency. A bandpass filter at the output of the modulator is centered at the upper sideband, $35,000 + (30 + f_d)$ Mc. Some of the power from the simulator klystron is coupled to a balanced mixer where it is mixed with the upper sideband signal obtained from the modulator through the bandpass filter. With the simulator klystron frequency set at $(35,000 + f_d)$ Mc, the difference frequency at the output of the balanced mixer is 30 Mc. This 30 Mc difference-frequency signal is amplified in a wideband 30 Mc locking amplifier. The output signal from the locking amplifier is fed into a 30 Mc phase detector where it is compared to a 30 Mc reference signal from a stable crystal oscillator. When the simulator klystron is phase locked to the reference signal, the output at the phase detector is a DC signal proportional to the relative phase between the 30 Mc reference signal from the crystal oscillator and the 30 Mc difference-frequency signal, obtained by mixing the upper sideband reference signal and the simulator klystron output signal. This DC signal is fed to the simulator klystron reflector as a frequency-correction signal. The simulator klystron thus oscillates at $(35,000 + f_d)$ Mc, f_d Mc above the transmitted radar frequency. The frequency of the simulated doppler signal is set by varying the frequency of the modulation signal into the balanced modulator. The lock-in range of the phase-locking circuit is sufficient for the frequency of the simulated doppler signal to be varied from approximately zero to 4 Mc. The output of the simulator klystron is fed through an attenuator to a waveguide switch. At this point the power is measured and preset to any desired level. It is then fed to the simulator antenna through the alternate switch output. A precision attenuator in this branch is used for calibration of the radar.

70 Gc Radar System

The 70 Gc radar head is similar to the 35 Gc system in all respects except that, of course, appropriate 70 Gc components are used. Both the 35 and 70 Gc antennas are designed so that the usual far-field distance ($2D^2/\lambda$) is located at the radar reflector in the ballistic-range tank.

A block diagram of the 70 Gc doppler simulator is shown in Figure 4. The balanced modulator and bandpass filter combination, as used in the 35 Gc simulator, could not be used here to produce the upper sideband at $70,000 + (30 + f_d)$ Mc because a suitable filter was not available. Instead, a single sideband generator was designed for this purpose. The single sideband generator is adjusted to cancel the lower sidebands produced at the two crystal modulators by adjusting their relative phases to be in phase opposition. Reduction of the lower sideband to about 20 db below the upper sideband is adequate for present purposes. In all other respects the operation of the 70 Gc and 35 Gc doppler signal simulators is similar.

Radar Installation on the Ballistic Range

The layout of the two radars relative to the ballistic range is shown schematically in Figure 5, and a photograph of the equipment is shown in Figure 6.

The radar chamber consists of a 50-foot-long tank, 8 feet in diameter, located at the end of the ballistic range. The uprange end of the tank is lined with microwave absorbing material to minimize the effect of range wall reflections on the radars. The radar reflector, which is made of thin sheet aluminum, is suspended across the flight line at 45 degrees to the flight axis. The supporting framework is designed to enable the sheet to be mounted easily and accurately in position. The sheet is replaced after each firing.

As a matter of convenience, the radars, the recording oscilloscopes, and the doppler signal simulators are all placed at the same location near the dielectric radar window. The output of each simulator is transmitted to the calibration point through low-loss circular waveguide. Each calibration antenna and its associated waveguide are carried on a boom which can be pivoted to locate the antenna on the flight line at a known radar range, or along the side of the tank out of

the line of fire and out of the main radar beam. The calibration point is approximately 19 feet from the radar reflector.

Operation

Each radar is calibrated before each projectile flight. The radar beam is optically aligned along the flight axis and the calibration antenna is swung into position. The simulator klystron is phase locked to the transmitter klystron, and simulator power is transmitted downrange to the radar. The output of the radar doppler amplifier will be a sine wave, the frequency of which is the doppler frequency being simulated. The amplitude of this signal is proportional to the simulator power and the system sensitivity. The sensitivity of the entire radar system (including all insertion losses and diffraction effects, if any) can then be determined by a measurement of simulator power and output voltage on the oscilloscope. It has been found adequate to calibrate the radar, before each firing, at only one simulated doppler frequency. From time to time calibration over the entire doppler frequency spectrum is carried out. The response is essentially flat from 0.5 Mc to 6 Mc.

During the projectile's flight the oscilloscopes are triggered from points uprange of the radar reflector. With four recording channels per radar available, there is a great deal of flexibility and various combinations of gains and sweep rates may be used. The transmitter power is monitored continuously at the time of firing, and the absolute value is measured immediately after the firing.

Data Reduction

On a typical projectile flight the following information is available:

1. Position as a function of time (from shadowgraph chronograph stations).
2. Stability of the model (from shadowgraph stations).
3. Output voltage from the radar as a function of time. An example of this record is shown in Figure 7. In the upper trace the output voltage is shown in relation to projectile range in the ballistic range; in the lower trace a part of the upper trace is expanded to show the doppler waveform.
4. A calibration record, relating (at some particular simulated doppler frequency) the output voltage to the ratio of simulator power to transmitted power (P_C/P_T).

From the above data the radar cross section as a function of distance can be obtained.

To reduce this data, the first step is to convert the output-signal record from a function of time into a function of range. This is readily done by using the known velocity and known triggering point. The output voltage is then converted into radar cross section as follows. If the simulator power (P_C) is adjusted to produce some particular voltage E_O, and if E_O occurs on the radar record at some range R_O, then it can be shown that

$$\frac{\sigma}{\lambda^2} = \frac{4\pi}{\lambda^2} \frac{P_C}{P_T} \frac{G_C}{G_R} \frac{R_O^4}{R_C^2}$$

where σ is the radar cross section, λ is the wavelength, P_C is the simulator power for the output voltage E_O, P_T is the transmitter power (into the antenna terminals), G_C is the gain of the simulator antenna, G_R is the gain of the radar antenna, R_O is the radar range for which the output voltage is E_O, and R_C is the range of the simulator antenna. It should be noted that this is an inherently accurate method of calibration in that only the ratios P_C/P_T and G_C/G_R are required, obviating the necessity for absolute power measurements. Using the above formula and the calibration record, the radar record is converted to one of radar cross section as a function of range.

Performance

The performance of the radars can best be judged by the results. A critical test is to observe the flight of a body with a constant radar cross section, such as a sphere or a blunt body with zero angle of attack throughout the flight. An example of the latter type of flight has been seen in Figure 7. It will be noticed that the signal increases monotonically as the radar reflector is approached. Reduction of this type of record has shown that the radar cross section remains constant within 2 decibels over most of the radar range.

Both radars have been used to track bodies with radar cross sections of one to ten square wavelengths over the full 50 feet of flight. The most useful part of the range is found to be from the calibration point at 19 feet from the radar reflector to a point close to the reflector. As the model nears the radar reflector, it approaches the near field of the radar antenna. The practical significance of the near field is that the antenna gain decreases rapidly as the range decreases. For projectiles which are off the beam axis, the near field extends for greater distances and the gain decreases more rapidly. In any case, the near-field region is easily recognized by a rapid decrease in radar cross section toward the end of flight. Both the 35 and 70 Gc radar antennas were designed so that the near fields do not extend beyond the radar reflector for an on-axis projectile.

III. RADAR CROSS SECTION STUDY

Theory

The radar cross section of a body can be predicted theoretically in exact form if the tangential components of the electric and magnetic fields induced on the surface of the body by the incident radar wave are known exactly (see, for example, Mentzer[6]). In the practical situation, the exact fields are usually not known. Thus some method must be used to obtain approximate values of these fields when the body and the incident wave are specified. The well-known physical optics approximation is often used when the body is metallic. In essence, this approximation takes for the tangential induced fields on the surface of the body a magnetic and an electric field which are just equal and opposite, respectively, to the tangential components of the magnetic and electric fields of the incident wave. An integration of these fields over the illuminated surface of the body then gives the far-field scattered-wave intensity, from which the radar cross section is determined. To extend this theory to the case of plasma-covered metallic bodies, it has been assumed that the effect of the plasma layer is merely to change the phase and amplitude of these induced fields. If the layer is very thin this appears to be a reasonably valid approximation. The far-field scattered wave is then computed in the same manner as in the usual physical optics approach.

When this technique is applied to the case of a metal sphere covered by a thin axisymmetric plasma layer, the resultant integral for the nose-on backscattering radar cross section (σ) can be shown[7] to be

$$\frac{\sigma}{\lambda^2} = \frac{\pi^3 a^2}{4\lambda^2}\left|\int_{x=0}^{x=4a/\lambda}\left(R_{TM} - R_{TE}\right)\left(1 - \frac{x\lambda}{4a}\right)\right.$$
$$\left.\exp\left[+j\,4\pi\frac{h}{\lambda}\right]\exp\left[-j\,\pi x\left(1+\frac{h}{a}\right)\right]dx\right|^2$$

where R_{TM} and R_{TE} are the TM and TE mode reflection coefficients for a metal-backed plasma layer, given by

$$R_{TM} = \frac{R_{pTM} + e^{z}}{1 + R_{pTM}\,e^{z}}$$

$$R_{TE} = \frac{R_{pTE} - e^{z}}{1 - R_{pTE}\,e^{z}}$$

where R_{pTM} and R_{pTE} are given by

$$R_{pTM} = \frac{\left(1-\frac{\Omega_p^2}{1-j\Omega_c}\right)\left(1-\frac{x\lambda}{4a}\right) - \left[\left(1-\frac{x\lambda}{4a}\right)^2 - \frac{\Omega_p^2}{1-j\Omega_c}\right]^{1/2}}{\left(1-\frac{\Omega_p^2}{1-j\Omega_c}\right)\left(1-\frac{x\lambda}{4a}\right) + \left[\left(1-\frac{x\lambda}{4a}\right)^2 - \frac{\Omega_p^2}{1-j\Omega_c}\right]^{1/2}}$$

$$R_{pTE} = \frac{\left(1-\frac{x\lambda}{4a}\right) - \left[\left(1-\frac{x\lambda}{4a}\right)^2 - \frac{\Omega_p^2}{1-j\Omega_c}\right]^{1/2}}{\left(1-\frac{x\lambda}{4a}\right) + \left[\left(1-\frac{x\lambda}{4a}\right)^2 - \frac{\Omega_p^2}{1-j\Omega_c}\right]^{1/2}}$$

and z is given by

$$z = -j\,\frac{4\pi h}{\lambda}\left[\left(1-\frac{x\lambda}{4a}\right)^2 - \frac{\Omega_p^2}{1-j\Omega_c}\right]^{1/2}$$

and λ is the radar wavelength, a is the radius of the sphere, and h is the thickness of the plasma layer. The plasma properties are defined by the normalized plasma frequency Ω_p and the normalized electron collision frequency Ω_c, which are

$$\Omega_p = \frac{\omega_p}{\omega} = \frac{1}{\omega}\left(\frac{q^2 N}{\epsilon m}\right)^{1/2}$$

$$\Omega_c = \frac{\nu_c}{\omega}$$

where ω is the radar angular frequency ($2\pi f$), ν_c is the electron collision frequency, ω_p is the plasma frequency, q is the electric charge carried by an electron and m is its mass, N is the electron number density, and ϵ is the capacitivity of freespace. It can be shown that if the reflection coefficients of the layer are not functions of the angle of incidence, the above integral can be explicitly evaluated in closed form. This is not the case for a plasma layer. Consequently, the integral must be evaluated numerically.

In this formulation of the scattering problem two mechanisms that can cause a decrease in the radar cross section are incorporated. The first is real power absorption in the plasma layer that occurs when the electron collision frequency is large (losses are present), the plasma frequency is nearly equal to the radar frequency, and the layer is sufficiently thick. Under the appropriate combination of these three variables, the plasma

layer becomes a matched lossy absorber coating on the metal body and very little power is scattered away from the body. The combination of parameters required for this to occur, for normal incidence of a plane wave on a plane plasma-coated metal wall, is shown in Figure 8. This corresponds to the stagnation-point conditions required to eliminate the nose-on specular point contribution to the total radar cross section. It can be seen that there are multiple values (k = 1, 2, 3, ...) of parameter sets that produce total absorption. The thinnest layer (k = 1) that will produce this effect is thicker than approximately one-third the free-space wavelength of the radar wave.

The second mechanism that causes radar cross-section changes is the diffraction of the backscattered power due to gradients in the plasma in the direction parallel to the metal body surface. This effect can produce large decreases in the radar cross section with plasma layers as thin as one-tenth the free-space radar wavelength, with or without losses in the plasma, provided the plasma frequency is greater than the radar frequency at the stagnation point. This is most effectively demonstrated by Figures 9 and 10. These figures show the radar cross section of a metal sphere as a function of the amount of the sphere covered by a uniform thin layer of plasma. Figure 9 shows the change in the radar cross section as the layer becomes thicker. It can be seen that a layer only one-tenth of a wavelength thick is necessary to give appreciable changes in the radar cross section as the amount of angular coverage is changed. Figure 10 shows the change in the radar cross section as the electron density changes in a layer of constant thickness. A change in electron density from critical density to 100 times critical density is encompassed.

To test the validity of this theory, several experimental measurements have been made on the static model range with metal spheres and caps.[8] These measurements have shown that the theory is reasonably accurate, provided that one does not consider bodies which have a large extent of surface nearly parallel to the direction of incidence of the radar wave.

Application of Theory

In order to predict the radar cross-section changes to be expected in the ballistic-range studies, it is necessary to know the spatial variation of the electron density and collision frequency throughout the entire shock layer around the body. The computation of the numerical values of these quantities in the flow field is a very lengthy aerodynamic calculation. The flow-field calculation must be repeated at each speed and/or pressure for which the radar cross section is to be calculated. To avoid this much extensive work at the present time, we have taken some representative approximations of the flow-field properties for use in the preliminary radar cross-section calculations presented here. The thickness of the plasma layer was taken to be the thickness of the overdense region of the plasma sheath around the body. The electron density and collision frequency within this overdense region were taken to be the stagnation-region values for the speed and ambient pressure considered. In order to obtain the dependence of the radar cross section on body speed, the way in which this overdense region thickens and spreads over the body as a function of speed was interpolated from a limited number of flow-field calculations. The radar cross section was then calculated as a function of velocity for the ambient pressure used in the ballistic-range studies. The theoretical results are shown in Figure 11, along with the experimental data. It can be seen that significant fluctuations in the radar cross section, of the order of 16 decibels, are predicted.

The real significance of this theoretical calculation is that a very large decrease in the radar cross section is obtained with only a very thin (compared to the radar wavelength) plasma layer. The details of how the radar cross section varies with speed depend critically on the development of the ionization around the body. Thus very good flow-field calculations are needed before exact comparisons between the theoretical and experimental results can be made. Conversely, the measured effect is a sensitive indicator of the actual integrated flow-field properties.

Experimental Results

In the experimental program the range pressure was held constant and the projectiles were launched at the desired velocities. In the present set of experiments the pressure was 10 mm Hg. All launchings were carried out using a 20-mm-bore gun.

The air in the range was analyzed before arbitrarily selected firings, and was found to contain only constituents normally present in the ambient atmosphere. The constancy of the air properties is borne out by the reproducibility of results over long periods of time (six to twelve months).

The projectile used to obtain the results presented here was a cylindrical plastic body with a spherical copper nose of 13 mm radius. The purpose of the metallic nose was to simulate the radar cross section of a metallic sphere of the same radius over a sufficient range of aspect angles, and also to provide a situation in which, it was believed, the theory of electromagnetic wave interaction with the plasma would be well understood. This model was found to be reasonably

stable in flight. On most flights the oscillations were within ±10 degrees and on good flights they were within ±5 degrees. The extent to which this body, in the head-on aspect, resembles a metal sphere of the same nose radius was investigated by measuring the static radar cross section in the static radar facility, which has been described.(5) It was found that near the nose-on aspect the radar cross section varies with aspect angle by only a few decibels, and the mean value agrees closely with the sphere value. In particular, the variation of cross section for a ±10 degree aspect variation is within 3 db. It is evident that this body resembles a metallic sphere quite closely if the oscillations during flight are small.

Results of flights observed with the 35 Gc doppler radar are shown in Figure 11. The spread of the data is almost entirely due to inflight oscillations of the model. Taking into account the fact that the minimum radar cross section for the static model occurs at head-on aspect, the most probable value for the inflight cross section is the smallest value. Results obtained on stable firings with negligible oscillation confirm this. At the minimum radar cross-section condition, the signal was close to noise and the actual maximum decrease could be greater than indicated. The theoretical prediction, which was discussed in a previous section, is also shown. The agreement between the theoretical prediction and the experimental measurements is apparent.

Results similar to those shown in Figure 11 have also been obtained with the 70 Gc radar.

IV. CONCLUSIONS

Millimeter radar instrumentation suitable for studying the effects of the plasma sheath associated with hypersonic flight on the radar cross section of projectiles in a free-flight ballistic range has been successfully constructed and operated. Several novel features, particularly a wire-grid beam splitter and a doppler signal simulator, permit simultaneous continuous coaxial-beam CW operation at two frequencies with high absolute accuracy. This equipment has been useful in exploring an interesting plasma effect: the reduction of the radar cross section of a plasma-sheathed metal body when the plasma becomes overdense.

A theoretical model that quantitatively predicts and explains the changes in radar cross section caused by a thin plasma layer over a metal body has been formulated. Comparisons between the predictions of this theory and the measured effects on hypersonic projectiles in a free-flight ballistic range show good correlation.

The change in the nose-on backscattering radar cross section of a metal blunt-nosed body when a thin shock-produced layer of ionized gas covers the body serves as a sensitive indicator of the spatial distribution of ionization in the bow-shock region. This phenomenon, when more fully explored, may hold promise as a new flow-field diagnostic technique.

V. REFERENCES

1. H.M. Musal, Jr., P.E. Robillard and R.I. Primich, "Radar Absorption Effects Measured in a Flight Physics Range," Technical Report TR62-209B, December 1962, GM Defense Research Laboratories, General Motors Corporation, Santa Barbara, California.

2. M. Gravel, "Interim Report on the Interaction of Microwaves with the Shock Front of Hypersonic Projectiles," CARDE Technical Report 466, August 1963, Canadian Armament Research and Development Establishment, Valcartier, P.Q., Canada.

3. R.I. Primich, "Microwave Techniques for Hypersonic Ballistic Ranges," in Electromagnetic Effects of Re-entry, Pergamon Press, 1961, pp. 186–195.

4. H.M. Musal, Jr., "Plasma Frequency and Electron Collision Frequency Charts for Hypersonic Vehicle Equilibrium Flow Fields in Air," Technical Report TR62-209C, December 1962, GM Defense Research Laboratories, General Motors Corporation, Santa Barbara, California.

5. W.E. Blore, P.E. Robillard and R.I. Primich, "35 and 70 Gc CW Balanced-Bridge Model Measurement Radars," Microwave Journal, to be published.

6. J.R. Mentzer, Scattering and Diffraction of Radio Waves, MacMillan Company, New York, 1955.

7. H.M. Musal, Jr. and W.E. Blore, "The Radar Cross Section of Dielectric-Coated Metal Bodies," GM Defense Research Laboratories Technical Report, in preparation.

8. W.E. Blore and H.M. Musal, Jr., "The Radar Cross Sections of Metal Hemispheres, Spherical Segments, and Partially Capped Spheres," Technical Report TR64-39, June 1964, GM Defense Research Laboratories, General Motors Corporation, Santa Barbara, California.

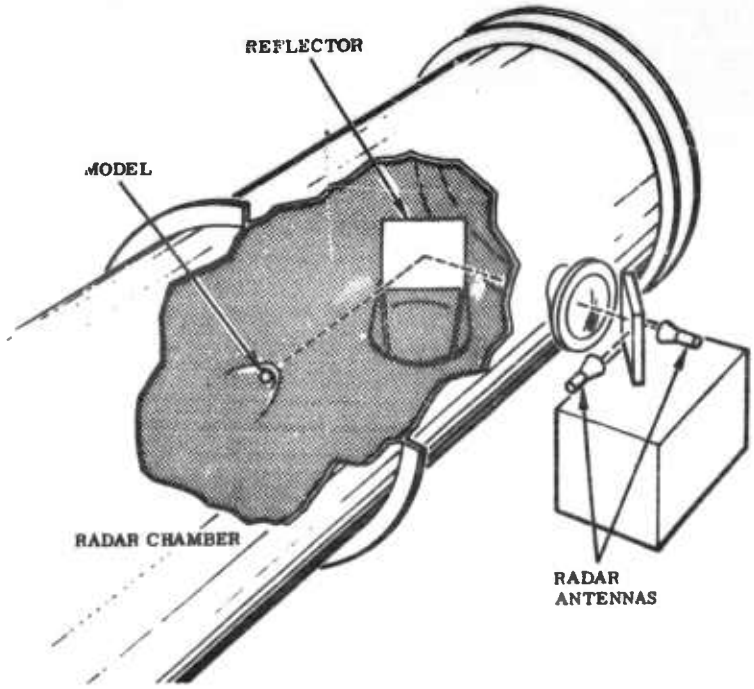

Figure 1 Head-On CW Doppler Radars

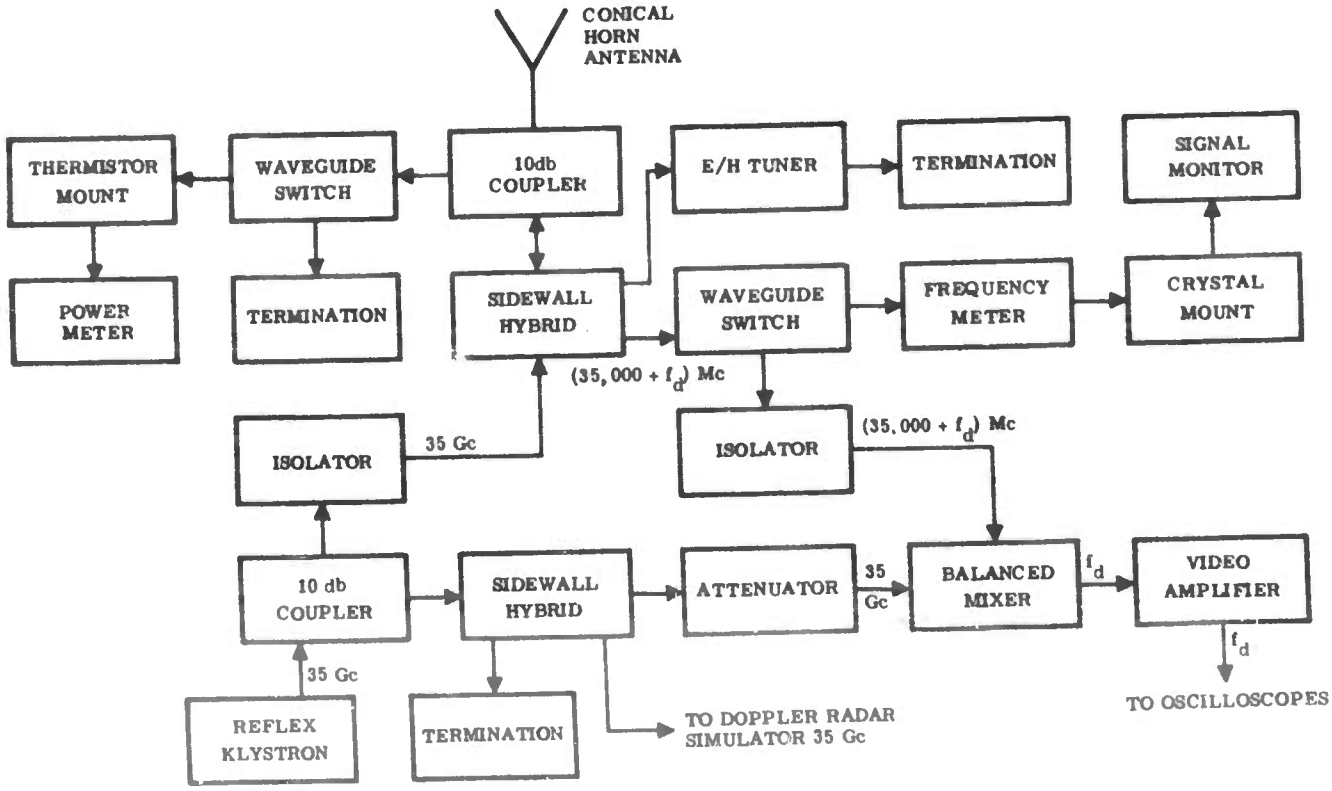

Figure 2 35 Gc CW Doppler Radar-Microwave Head

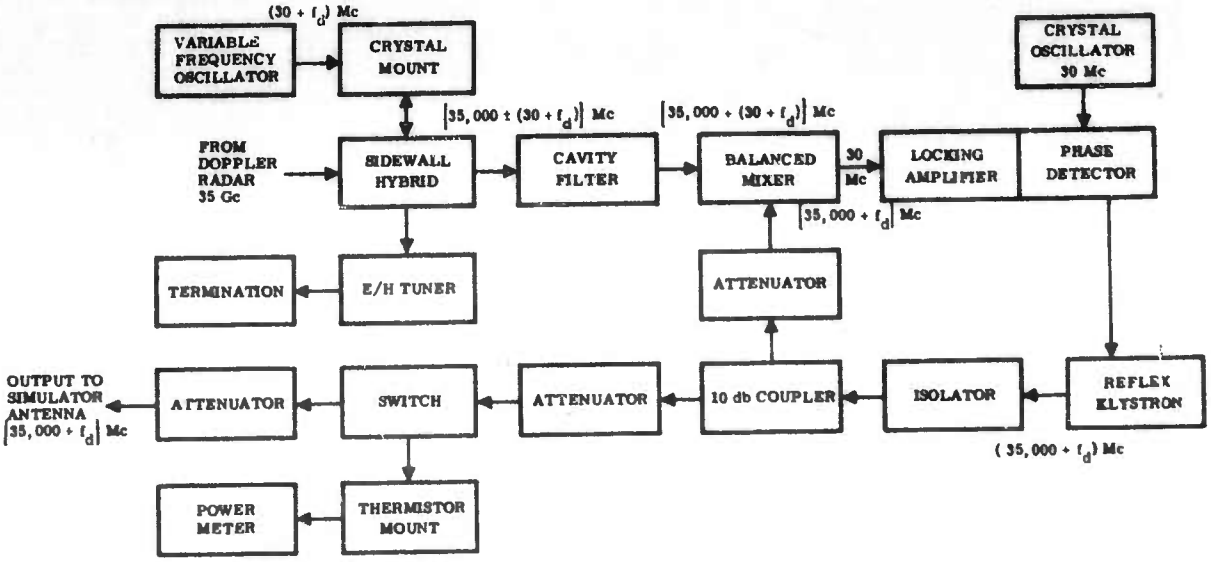

Figure 3 35 Gc CW Doppler Radar-Doppler Simulator

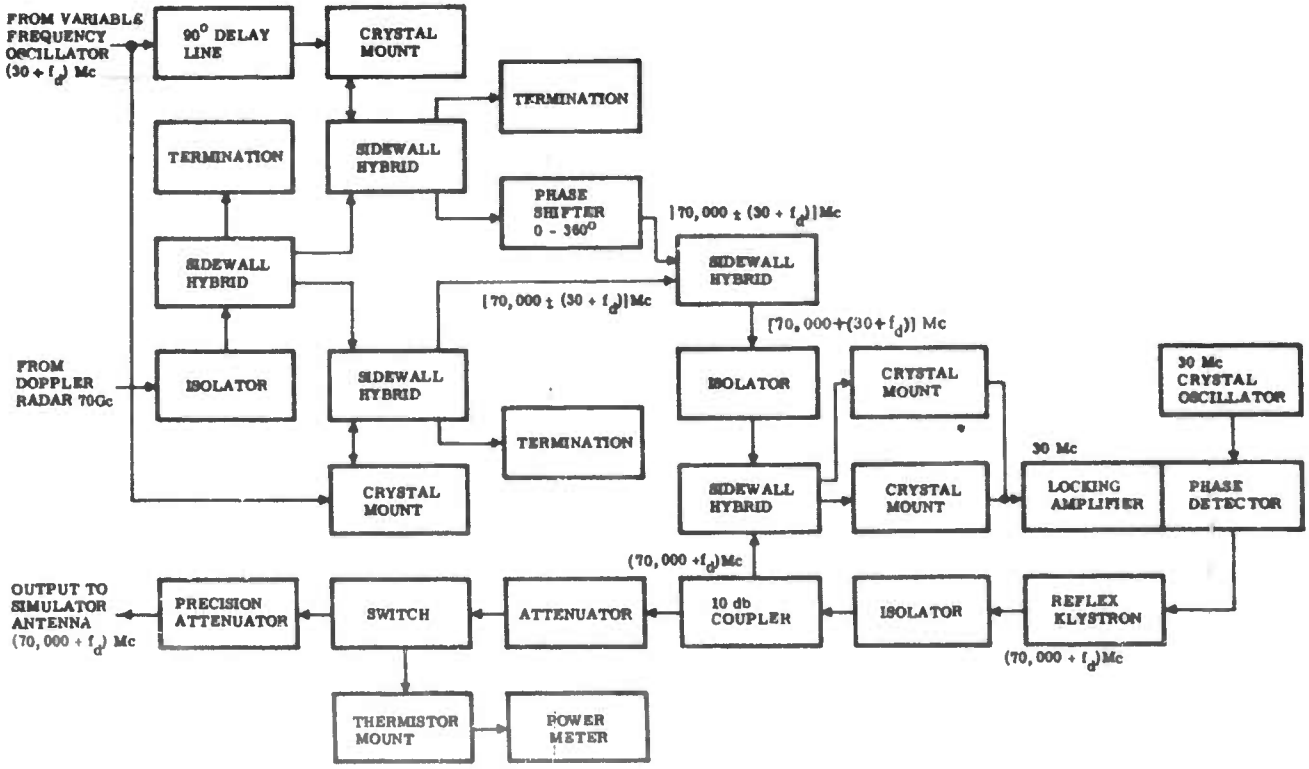

Figure 4 70 Gc CW Doppler Radar-Doppler Simulator

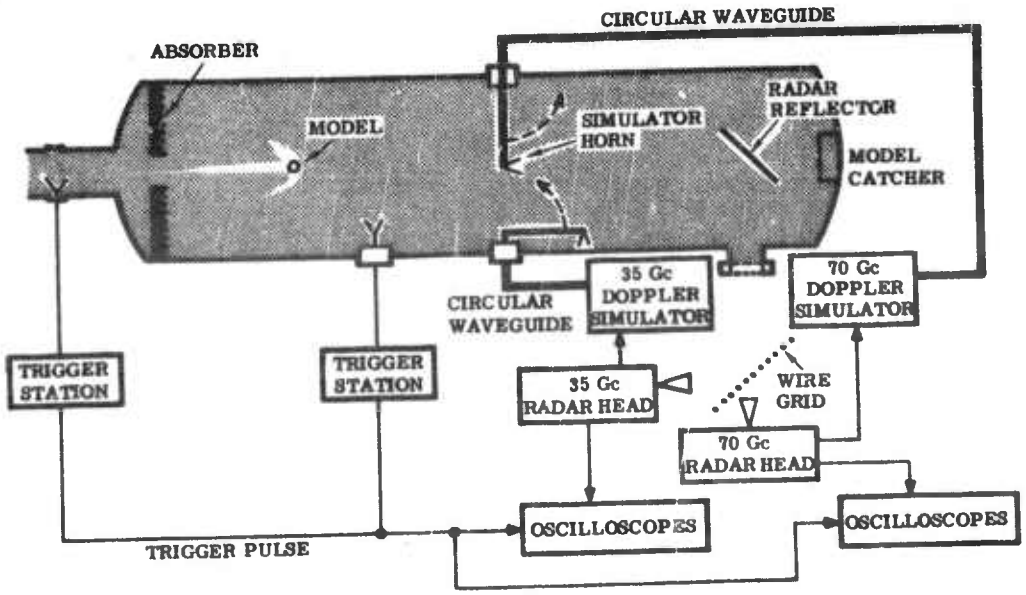

Figure 5 Radar Installation on the Ballistic Range – Schematic

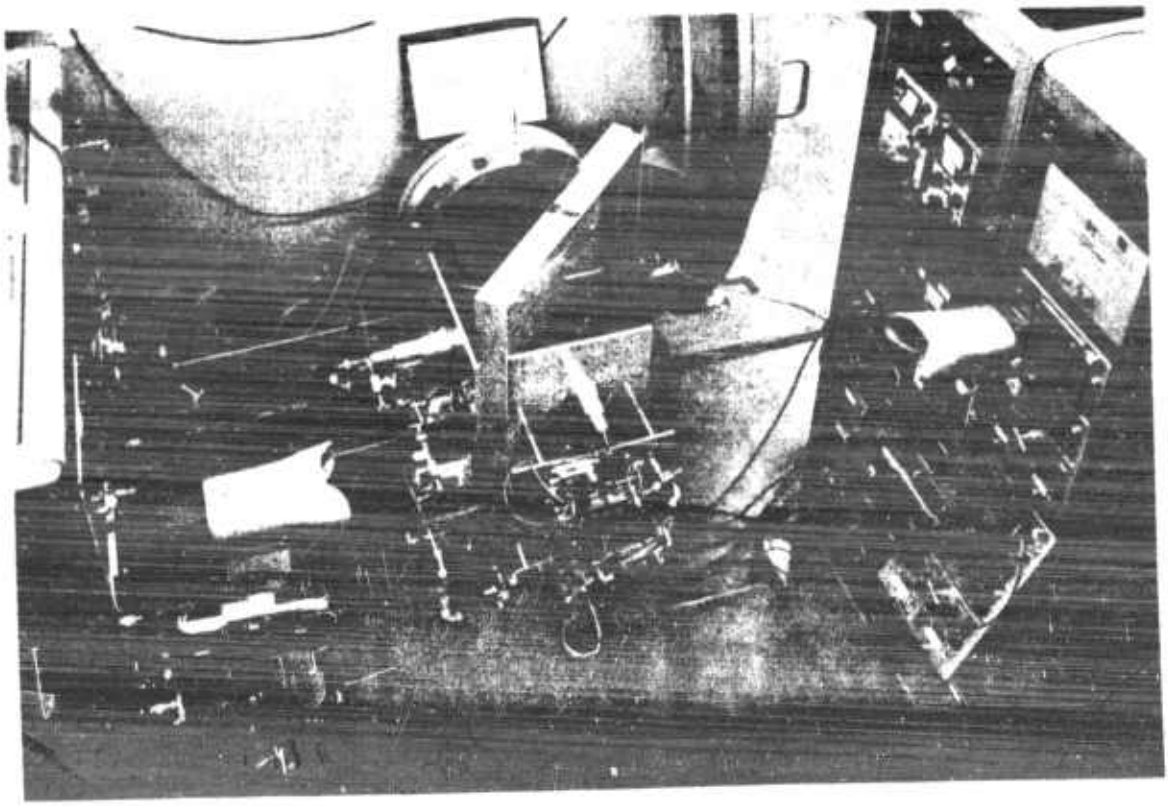

Figure 6 Radar Installation on the Ballistic Range

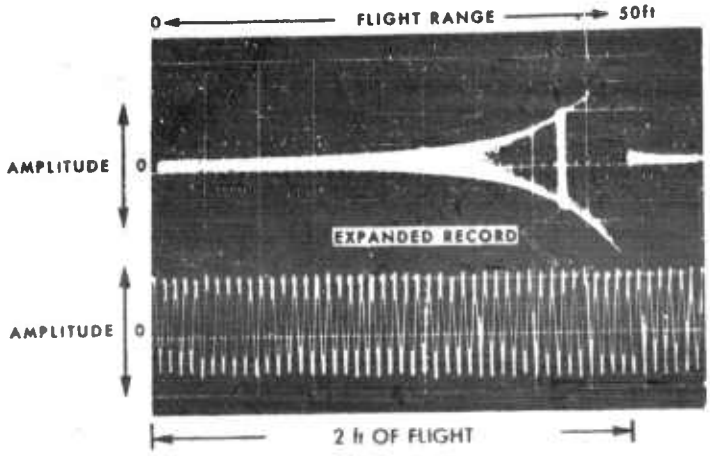

Figure 7
Typical Doppler Radar Record

Figure 8(a)
Required Plasma Frequency

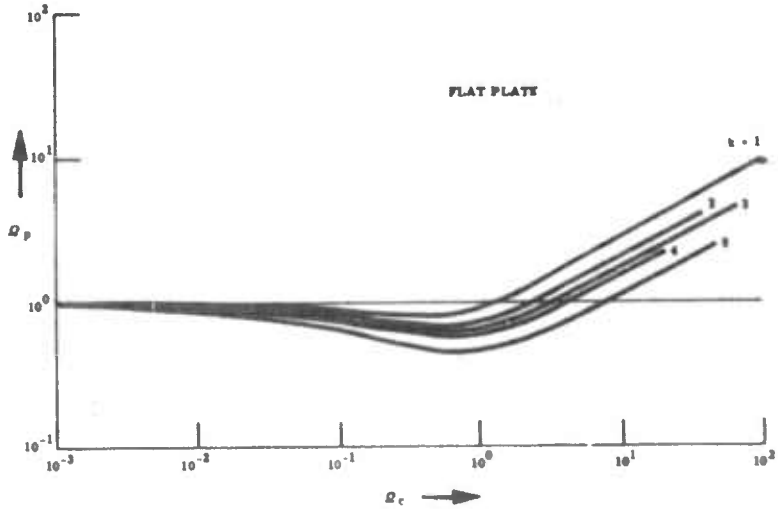

Figure 8(b)
Required Thickness

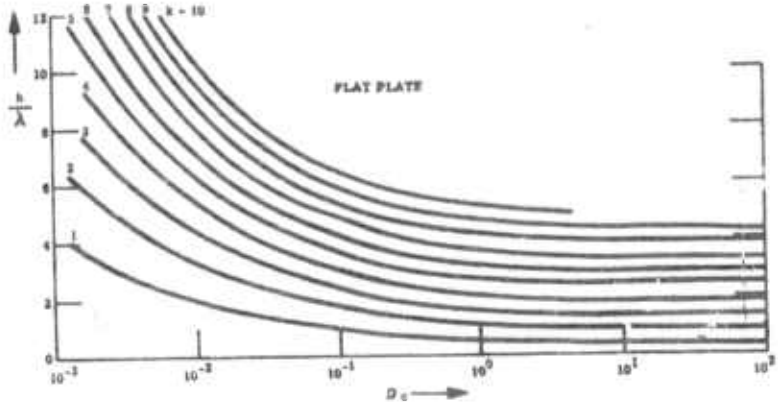

Figure 8 Conditions Required for Zero Reflection from a Uniform-Plasma Coated Flat Metal Wall

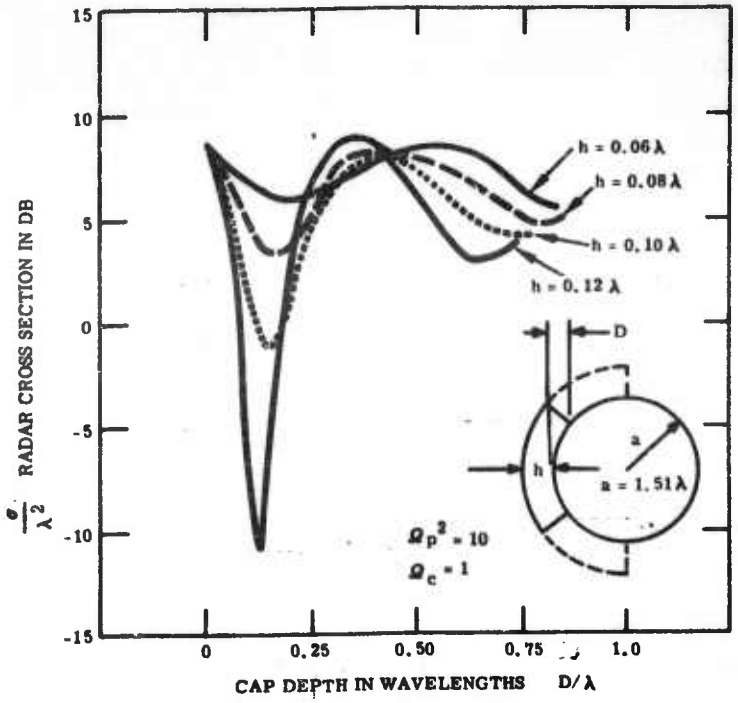

Figure 9 Nose-On Backscattering Radar Cross Section of a Plasma-Covered Metal Sphere: Effect of Plasma Thickness

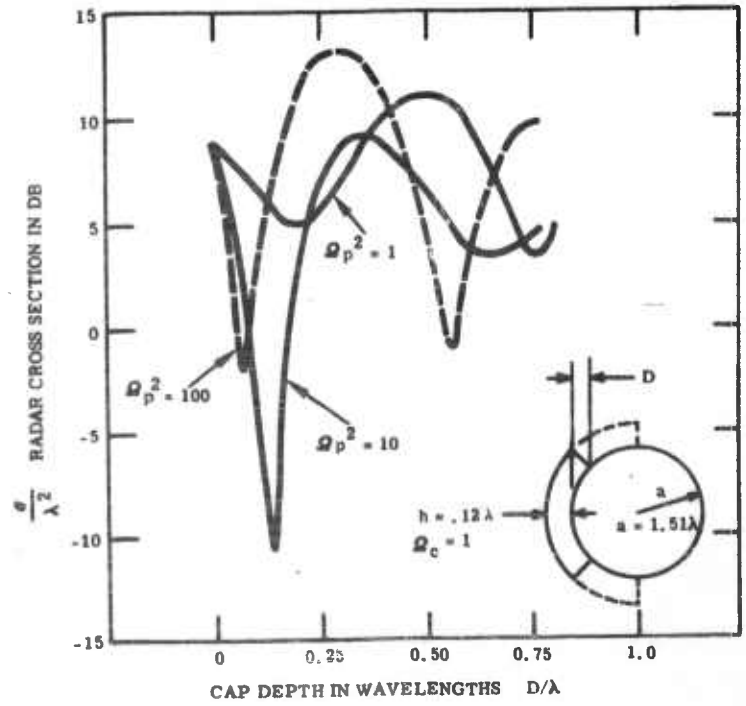

Figure 10 Nose-On Backscattering Radar Cross Section of a Plasma-Covered Metal Sphere: Effect of Plasma Density

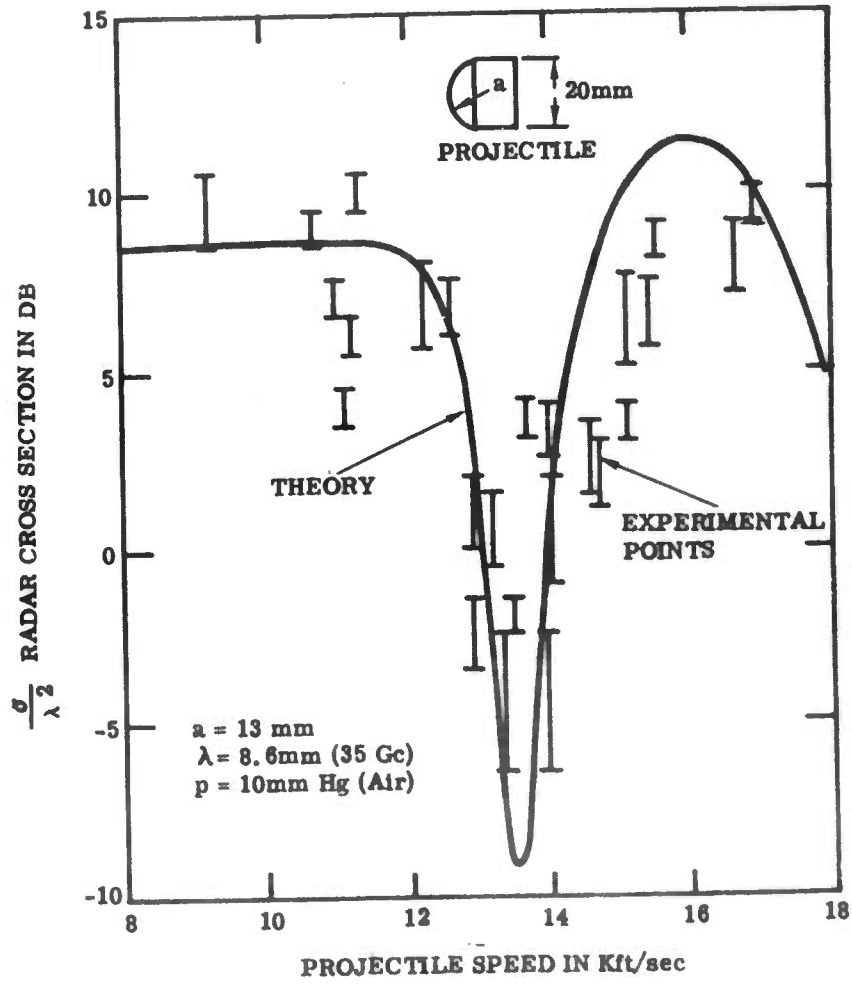

Figure 11 Radar Cross-Section Changes in Ballistic Range Compared to Theory

UNCLASSIFIED